Loss-Induced Confinement in Photonic Crystal Vertical-Cavity Surface-Emitting Lasers

Dominic F. Siriani, *Student Member, IEEE*, Paul O. Leisher, *Member, IEEE*, and Kent D. Choquette, *Fellow, IEEE*

***Abstract*—Through calculations and comparison with experimental results, we verify that loss introduced by an etched photonic crystal in a vertical-cavity surface-emitting laser (VCSEL) contributes significantly to the transverse optical confinement and supported modes. The optical loss is examined theoretically using a simple waveguide model from the scalar Helmholtz equation. The modal loss of fabricated lasers is extracted from the observed spectral-mode splitting. The effect of modal loss on the slope efficiency and modal behavior is examined. The model is found to be consistent with experimental measurements, and provides a means of accurate design of single-mode photonic crystal VCSELs.**

***Index Terms*—Distributed Bragg reflector lasers, laser modes, semiconductor lasers.**

I. Introduction

VERTICAL-CAVITY surface-emitting lasers (VCSELs) are useful for a variety of applications, particularly as a source for short-range optical communication and position tracking. VCSELs have advantages over other semiconductor lasers in many characteristics, including low-power operation, low-cost and high-volume manufacturing, on-wafer testing, and the support of only a single longitudinal optical mode. However, VCSELs tend to operate in many transverse modes, while for many VCSEL applications a single-transverse-mode device is desired.

In seeking a single-mode VCSEL, several different transverse optical confinement approaches have been investigated. These structures include oxide apertures [1], proton-implanted apertures [2], oxide/implant hybrid structures [3], surface relief etched lasers [4], [5], photonic crystal patterns [6]–[11], and etched holey patterns [12], [13]. For oxide, proton-implanted, and hybrid VCSELs, correlations have been made between the spectral-mode characteristics and the induced refractive index contrast arising from the transverse confinement structure created by the cavity confinement [14]–[16]. In these previous studies, optical loss is neglected because of its assumed insignificant role in confinement. However, recent work has suggested that in etched holey and photonic crystal structures, loss can have a significant effect on the mode structure [17]. In fact, it has been shown that loss to higher order modes can be responsible for single-mode operation in photonic crystal VCSELs [18].

There are many theoretical approaches for determining the transverse modes of VCSELs with various transverse optical confinement structures [19]. The method presented here employs a simple cylindrical waveguide analysis. From this approach, the laser emission wavelength and transverse-mode spacing can be determined [20], although optical loss has not previously been incorporated into this model. Other models, including a vector mode-matching method [21], have been used to calculate mode structures that incorporate loss, such as in oxide, ion-implanted, and hybrid VCSELs [22]. Direct numerical 3-D and vectorial modeling [15], [23], [24] is also capable of determining the modes of photonic crystal VCSELs but is not conducive to rapid device design.

The effect of loss on the transverse confinement in VCSELs is investigated through finite-difference calculations performed by incorporating a complex index for the lossy cladding region taken to be the photonic crystal that surrounds the lasing defect cavity. In this study, the loss considered is classified broadly as scattering and diffraction from the photonic crystal holes etched partially through the laser cavity. Lasers operating in both single-modeand multimode emission are simulated, where the single-mode VCSELs have a measured $>$30 dB side mode suppression ratio for all higher order modes. The results of calculations are compared to experimental spectral measurements from fabricated photonic crystal proton-implanted VCSELs. The results of the comparison between theory and experiment reveal the validity of modeling a photonic crystal as a lossy structure.

The method presented here is a semiempirical approach that uses comparison to experimental data. Calculations using the lossy model are developed using the experimental spectral splitting between the fundamental and first-order modes, and the results are then used to predict higher order spectral-mode splitting. Comparisons between the calculated modal loss and both the expected trend with etch depth and the measured slope efficiency further validate the lossy model. Finally, an analysis of the calculated normalized frequency V_{eff} and modal loss of studied lasers is presented as a more complete characterization of single-mode lasing operation and can enable accurate design of single-mode photonic crystal VCSELs.

Manuscript received September 04, 2008; revised November 21, 2008. Current version published May 28, 2009. This work was supported in part by the National Defense Science and Engineering Graduate (NDSEG) fellowship.

D. F. Siriani and K. D. Choquette are with the Electrical and Computer Engineering Department, University of Illinois at Urbana-Champaign, Urbana, IL 61801 USA (e-mail: siriani@illinois.edu; choquett@illinois.edu).

P. O. Leisher was with University of Illinois at Urbana-Champaign, Urbana, IL 61801 USA. He is now with nLight Corporation, Vancouver, WA 98665 USA (e-mail: pleisher@ieee.org; paul.leisher@nlight.net).

Color versions of one or more of the figures in this paper are available online at http://ieeexplore.ieee.org.

Digital Object Identifier 10.1109/JQE.2009.2013124

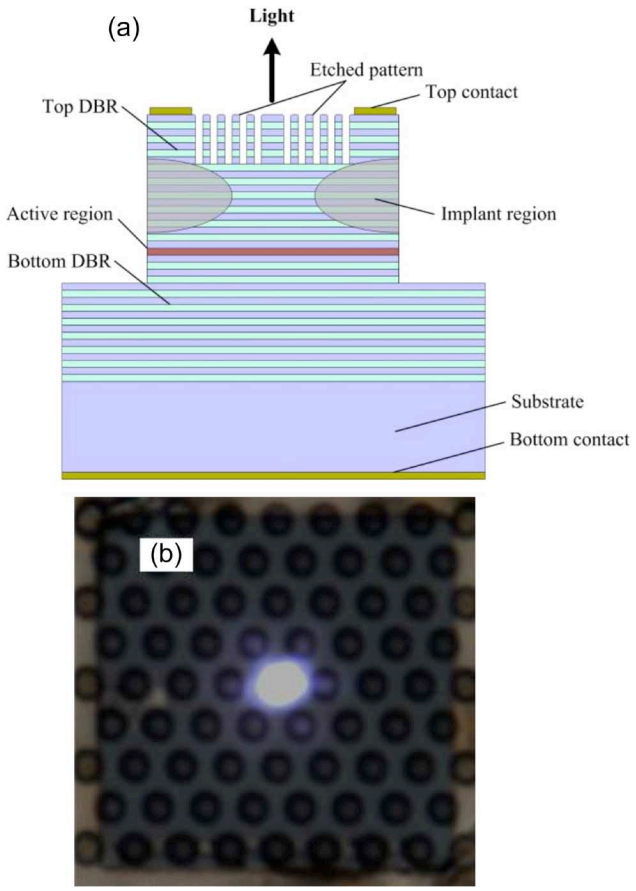

Fig. 1. (a) Photonic crystal VCSEL cross section. (b) Top view of a fabricated photonic crystal VCSEL while lasing.

II. Photonic Crystal VCSEL Design

The devices under investigation are ion-implanted photonic crystal VCSELs operating at nominally 850 nm [13]. The lasers are multiple quantum well devices grown by metal–organic chemical vapor deposition with 20 top distributed Bragg reflector (DBR) mirror periods. The VCSELs are mesa structures with a 20-μm implant aperture in the top mirror. This large implant aperture size is chosen so that the thermal lens created is essentially uniform across the much smaller photonic crystal defect aperture. Following the implantation, a pattern of circular holes is defined by electron beam or optical lithography [25] and etched into the top DBR to form the photonic crystal. Fig. 1(a) shows a cross section of this VCSEL design. In these lasers, the ion-implanted region is used for electrical confinement, and a photonic crystal with a defect aperture smaller than that of the implanted region provides the optical index confinement.

As shown in Fig. 1(b), the photonic crystal pattern is a hexagonal array of circular holes. A single missing hole in the center of the pattern is the defect that forms the optical aperture. Several parameters of the photonic crystal region are varied such that a total of 46 VCSELs are characterized. The hole period (referred to here as a) varies from 2 to 7 μm in 0.5-μm steps. The ratio of the hole diameter (b) to the hole period (b/a) is fixed at 0.6 and 0.7. Finally, the depth of the photonic crystal holes are varied using three different etch times. The etch depth dependence on hole diameter is determined through a fit to several experimental values, as seen in Fig. 2, which allows for the extrapolation of all depths used in this study. All of these parameters serve to alter the waveguiding properties of the photonic crystal.

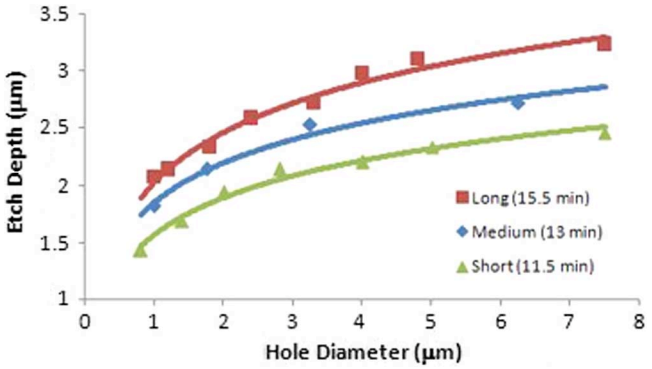

Fig. 2. The etch depth dependence on hole size for three different etch times investigated. Points are measured values and lines are fits to those values.

III. Lossy Photonic Crystal Model

To find the properties of an index-guided VCSEL, an effective index approach can be used [26], [27]. In previous analyses of photonic crystal VCSELs [28], an effective waveguide approach [29] outlined in Fig. 3 was used to identify the number of lasing modes. An effective refractive index is found for the photonic crystal cladding region using a photonic band diagram analysis. The plane-wave-expansion method is used to find the effective refractive index for each of the DBR layers penetrated by the photonic crystal, and then these indices are used in a transmission matrix calculation to find the resonances and effective indices for the entire DBR structure. The VCSEL is modeled as a cylindrical step-index optical fiber. Knowing the core and cladding refractive indices, it is possible to apply waveguide analysis to find the mode cutoff. The mode cutoffs are determined by a normalized frequency V_{eff} parameter defined by [29]

$$V_{\text{eff}} \approx \frac{2\pi a}{\lambda}\sqrt{n_{\text{core}}^2 - n_{\text{clad}}^2} \tag{1}$$

where a is the core radius, λ is the lasing wavelength, and n_{core} (n_{clad}) are the refractive indices in the core (cladding) region. The single-mode condition can be found to be [29]

$$V_{\text{eff}} < 2.405 \tag{2}$$

where no optical loss is assumed.

In order to introduce loss created by the photonic crystal, we wish to use a complex refractive index [30]. In such a model, the traditional V_{eff} method cannot be applied. Additionally, it is possible and often observed that a laser cavity can support multiple modes but only one lases. Since we seek to design single-mode lasers, even for multimode cavities, we must take a different approach. Thus, a finite-difference approach is used to solve for

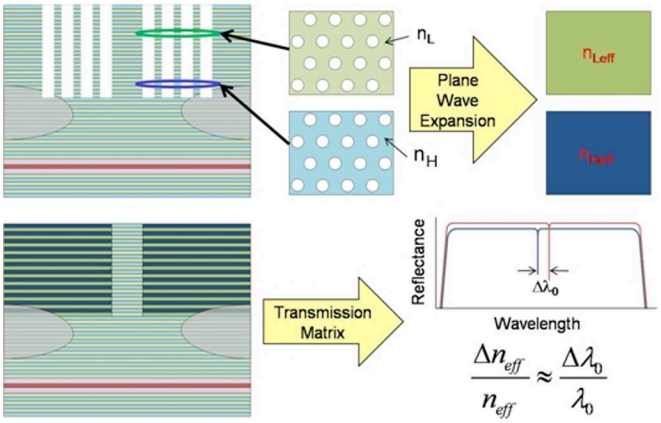

Fig. 3. A flowchart of the procedure used to find (the real part of) the effective refractive index of the photonic crystal cladding in the step-index model.

VCSEL modes from solutions to the scalar Helmholtz equation given by

$$\nabla^2 U(r,\phi,z) + n^2(r)k_0^2 U(r,\phi,z) = 0 \tag{3}$$

where U is the field profile, n is the refractive index profile, and k_0 is the wavenumber. In this model, a cylindrical waveguide is assumed with solutions

$$U(r,\phi,z) = u(r)e^{-im\phi}e^{-i\beta z} \tag{4}$$

where m is an integer and β is the propagation constant given by $2\pi/L$ (L is the longitudinal cavity length). Inserting (4) into (3) gives the 1-D differential equation

$$\frac{d^2u}{dr^2} + \frac{1}{r}\frac{du}{dr}\left(n^2(r)k_0^2 - \beta^2 - \frac{m^2}{r^2}\right)u(r) = 0. \tag{5}$$

Although this equation can be solved analytically with a complex refractive index, as is mentioned next, we use an iterative fit to experiment, which is more easily implemented using a finite-difference solution method. Taking a finite-differences approach transforms (5) into an eigenvalue problem with eigenvalues (mode resonances) given by k_0 and eigenvectors (mode profiles) given by u [31], which is expressed as

$$\left[\frac{u_{j+1} - 2u_j + u_{j-1}}{(\Delta r)^2} + \frac{1}{r_j}\frac{u_{j+1} - u_{j-1}}{2\Delta r} - \left(\beta^2 + \frac{m^2}{r^2}\right)u_j\right] = -n_j^2 k_0^2 u_j \tag{6}$$

where j is an index associated with a point in space.

The variable parameters that determine the solutions to (6) are the core and cladding refractive indices. In our simulations, the core refractive index is taken as entirely real (no loss) and fixed at the value 3.5. For the cladding, the real part of the refractive index is calculated as discussed before (see Fig. 3), which explicitly accounts for the etch-depth dependence [8].

The inclusion of a complex refractive index

$$n_{\text{clad}} = n'_{PhC} + in''_{PhC} \tag{7}$$

in (6) will imply that the field eigenvector and the wavenumber also will be complex. Since the aim of the calculation is to obtain the resonant wavelengths, the complex wavenumber is of interest. The resonant wavelength can be extracted from the wavenumber:

$$k_0 = \frac{\omega_0}{c} = \frac{2\pi}{\lambda_0}. \tag{8}$$

The real-valued resonance must be found by taking

$$\lambda_0 = \frac{2\pi c}{\text{Re}\{\omega_0\}} = \frac{2\pi}{\text{Re}\{k_0\}} \tag{9}$$

and the loss (in inverse length) can be found from

$$\alpha_i = \text{Im}\{k_0\} \tag{10}$$

where α_i is defined to be the amplitude loss (this factor is multiplied by 2 for intensity-based loss). In our model, we incorporate a complex refractive index only for the cladding region. We thus neglect differences of modal gain from the active region. This is justified because the gain cross section area for our devices defined by implantation is always much larger than the optical cavity defined by the photonic crystal defect.

Fig. 4(a) shows the calculated mode spectra using (6) for a photonic crystal VCSEL. The particular design considered is a single-mode laser ($a = 4.5$ μm, $b/a = 0.6$, and $V_{\text{eff}} = 1.585$) when loss is not included. As is apparent in Fig. 4(a), as the imaginary component of the refractive index in the cladding region becomes nonzero, higher order modes subsequently appear which shift to shorter wavelength, consistent with increased confinement induced by optical loss of the photonic crystal region [30]. The increased loss also leads to greater mode intensity in the core region, thus altering the radial mode profile u.

Following [16], our next comparison is the transverse-mode splitting for multimode lasers to determine the influence of the cladding loss on the transverse-mode splitting. Fig. 4(b) shows the calculated spectral splitting between the fundamental and first higher order modes for lossless and lossy cases. For this calculation, a constant cladding index of 3.495 (a hypothetical value appropriate for typical photonic crystal patterns) is used, and an imaginary part of 0.05 is included for the lossy case. Fig. 4(b) illustrates that for small apertures the introduction of loss into the cladding has a significant effect on the spectral splitting. This size dependence is expected since smaller cavity diameter implies that the modes extend a greater amount into the photonic crystal cladding region. In summary, Fig. 4 demonstrates that using a complex refractive index for the photonic crystal cladding region significantly changes the modal properties of the laser. The imaginary component of the cladding refractive index can thus be extracted from the spectral characteristics of the laser cavity.

IV. Experimental Results

In this section, we first extract the modal loss using the measured spectral splitting between the modes. Solving (6) for the fundamental and first higher order mode resonances, and then fitting to the experimental spectral splitting between the modes

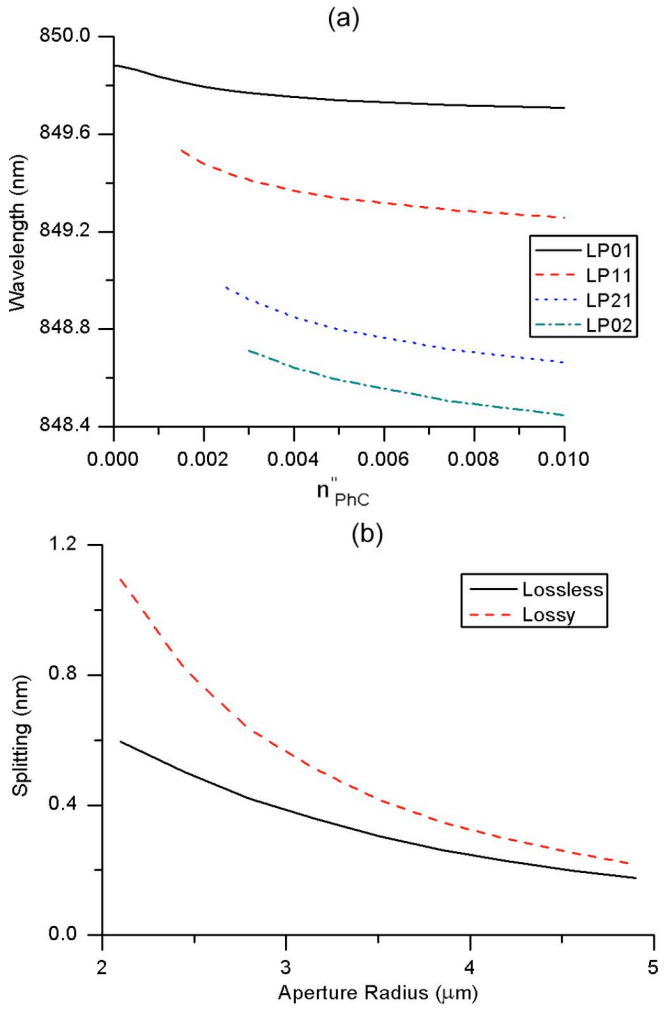

Fig. 4. (a) Resonance wavelength of modes as a function of the imaginary part of the complex cladding refractive index. (b) Calculated transverse-mode spectral splitting between fundamental and first higher order modes versus aperture radius for lossless and lossy photonic crystal cladding.

is used to determine the value for the imaginary part of the cladding refractive index. These values are then compared to the slope efficiency and the modal characteristics of VCSELs with various photonic crystal designs and etch depths to show our model is self-consistent.

In our experimental procedure, we first determined the threshold current and slope efficiency of the VCSELs using a semiconductor parameter analyzer. We then use cold-cavity spectral measurements from an optical spectrum analyzer. Spectra were measured below threshold current (approximately 0.9 times threshold) in order to avoid thermal effects. As previously mentioned, this analysis can only be performed on cavities supporting more than one mode. It is important to clarify that all tested devices have cavities that support multiple modes. However, we will refer to "single-mode lasers" as devices that operate only in the fundamental mode with power at least 30 dB above any higher order modes or noise up to maximum output power. Therefore, single-mode lasers may have a laser cavity that supports multiple modes but only the fundamental mode lases.

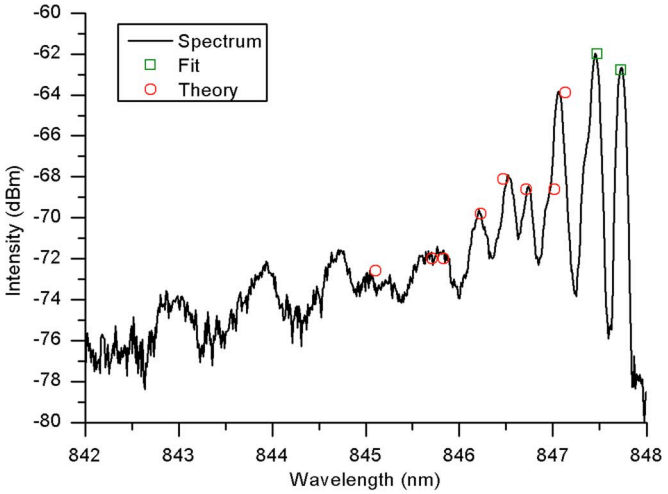

Fig. 5. Subthreshold spectrum for a particular photonic crystal VCSEL (periodicity of 6.5 μm and b/a of 0.7) with theoretical calculations of resonances shown by circles. The points used to fit the imaginary cladding index shown by two squares ($n_{\text{clad}} = 3.4968 + i0.0498$).

Fig. 5 shows a typical example comparison of theory and experiment for a particular photonic crystal VCSEL spectrum. The laser tested has a photonic crystal with $a = 6.5$ μm, $b/a = 0.7$, and an etch depth of 2.94 μm. Using the method outlined before with a core refractive index of 3.5, we found the cladding refractive index to be approximately $3.497 + i0.05$. In Fig. 5, the open squares are the points used to fit the experiment, and the open circles are the calculated resonances. This figure demonstrates that resonant wavelengths predicted from our model for higher order modes agree well with experimental data.

The etch depth of the photonic crystals should influence optical loss and thus is expected to affect the modal properties for these lasers. The mode overlap for a particular mode of a laser is taken as the percentage of the mode intensity that overlaps the cladding region. Fig. 6(a) shows the calculated mode overlap plotted against the etch depth, and Fig. 6(b) shows the calculated loss to the fundamental mode plotted against the etch depth. Fig. 6(a) shows that, generally, the mode overlap with the cladding region is larger for shallower etch depths. This result is expected since the photonic crystal will not prevent mode divergence, and thus, a larger amount of mode intensity exists in the cladding region [32]. Fig. 6(b) reveals that the modal loss also, generally, increases as the etch depth decreases. This result also can be deduced from the data of Fig. 6(a) since an increase in mode overlap with the cladding corresponds to an increase in the amount of loss the mode experiences. In phenomenological terms, the modal loss increases for decreasing etch depths since the photonic crystal will act more as a loss mechanism rather than a waveguide. These plots only take into account etch depth; the photonic crystal period and hole diameter will also influence the mode overlap and loss.

Another device parameter to evaluate loss is the laser slope efficiency. Optical loss is correlated to the slope efficiency by the proportionality

$$\eta_{\text{slope}} \propto \frac{\alpha_m}{\alpha_m + \alpha_i} \tag{11}$$

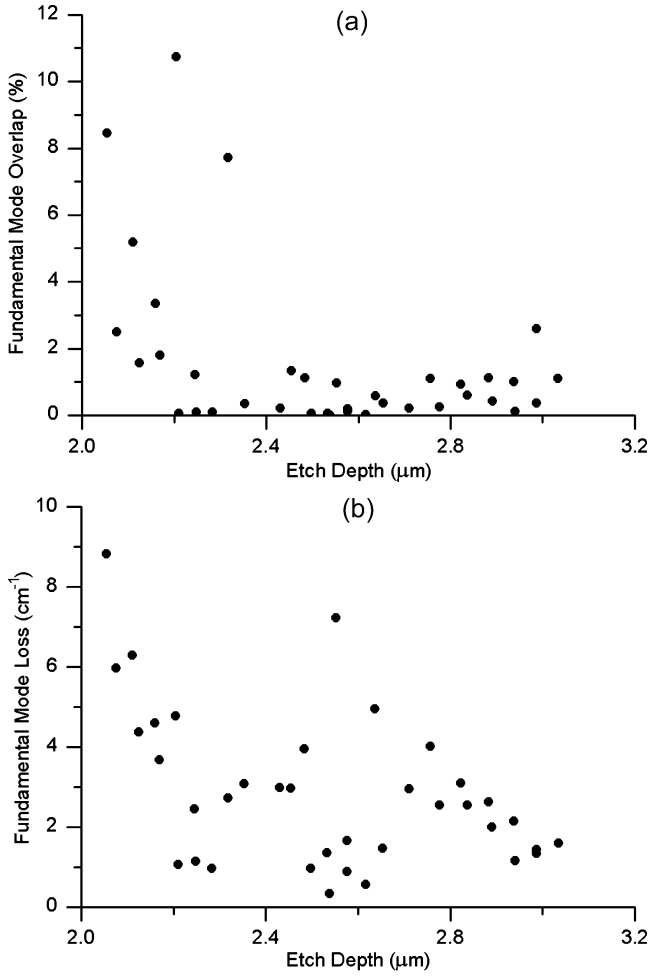

Fig. 6. (a) Percentage of the fundamental mode overlapping the cladding region. (b) Modal loss for the fundamental mode plotted against the etch depth.

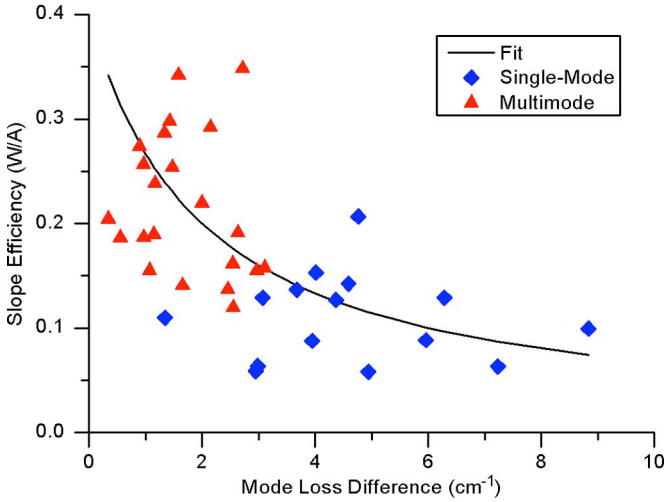

Fig. 7. The slope efficiency versus the fundamental mode loss. Single- and multimode devices are distinguished by diamonds and squares, respectively.

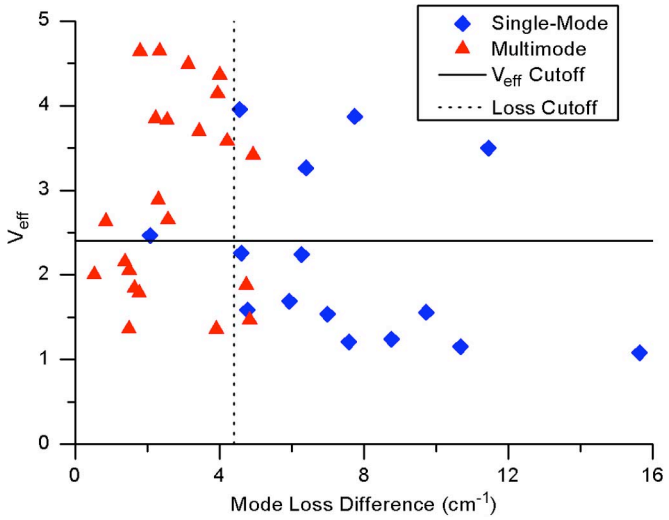

Fig. 8. V_{eff} and modal loss difference between the fundamental and first higher order modes for various photonic crystal VCSELs. The single-mode and multimode operations are indicated by diamonds and squares, respectively. The solid line indicates the single-mode cutoff condition for $V_{\text{eff}} = 2.405$. The dotted line indicates an empirical modal loss difference cutoff.

where α_m is the mirror loss and α_i is defined in (10). Fig. 7 shows the measured slope efficiencies plotted against the extracted modal losses for the fundamental mode for various photonic crystal VCSEL structures. Also shown in Fig. 7 is the expected slope efficiency obtained using (11), where a constant value of α_m fit to a single data point is used to determine the curve. Fig. 7 reveals that the experimental measurements of slope efficiency follow the trend indicated by our model. As the fundamental mode loss increases, the slope efficiency decreases, even for multimode devices. The distribution of the data around the line is the result of differences in mirror reflectivity, injection efficiency, and contributions from higher order modes.

Finally, we compare single-mode and multimode operation of these photonic crystal devices using our lossy model. In past study, the number of modes has been correlated to a V_{eff} parameter, which is dependent on the light wavelength, the core size, and the core/cladding index difference [28]. Here, we augment this correlation by using the calculated V_{eff} as well as the calculated modal loss. Fig. 8 illustrates the single-modeand multimode devices and their calculated V_{eff} (using only the real part of the refractive index) and the modal loss difference between the fundamental and first higher order modes. This modal loss difference is significant since it is related to whether the higher order mode achieves the gain necessary to achieve lasing. From Fig. 8, it can be seen that several single-mode devices lie above $V_{\text{eff}} = 2.405$ and several multimode devices lie below this cutoff. However, for sufficiently large values of modal loss, the photonic crystal VCSELs are single-mode regardless of their V_{eff} parameters. For a particular value of modal loss difference (approximately 5 cm^{-1}), there is a clear division between single-modeand multimode operation with few exceptions. This empirically deduced modal loss is comparable to the typical value of optical loss found in 850 nm VCSELs. Thus, loss plays a significant role in determining the number of lasing modes of a photonic crystal VCSEL device. Moreover, our lossy model enables a better prediction of the modal characteristics for the design of single-mode VCSELs.

V. Conclusion

Ion-implanted photonic crystal VCSELs with variable photonic crystal periods, hole sizes, and etch depths have been studied. A lossy model for the photonic crystal waveguide has been developed. We demonstrate that loss can have a significant role in the modal characteristics of etched photonic crystal VCSELs and, in fact, can be a primary mechanism of maintaining single-mode operation. Optical loss values for the photonic crystal are extracted from the transverse-mode splitting of fabricated devices. Comparisons of these modal losses with higher order mode splitting, effects of etch depth, slope efficiency, and single-modeor multimode operation serve to verify that the model is experimentally self-consistent and reveal the significant influence of loss on the confinement of photonic crystal VCSELs. This semiempirical approach can serve to aid in the design of high-efficiency, single-mode photonic crystal VCSELs.

References

[1] C. Jung, R. Jager, M. Grabherr, P. Schnitzer, R. Michalzik, B. Weigl, S. Muller, and K. J. Ebeling, "4.8 mW single-mode oxide confined top-surface emitting vertical-cavity laser diodes," *Electron. Lett.*, vol. 33, no. 21, pp. 1790–1791, 1997.

[2] R. A. Morgan, G. D. Guth, M. W. Focht, M. T. Asom, K. Kojima, L. E. Rogers, and S. E. Callis, "Transverse mode control of vertical-cavity top-surface-emitting lasers," *IEEE Photon. Technol. Lett.*, vol. 4, no. 4, pp. 374–377, Apr. 1993.

[3] E. W. Young, K. D. Choquette, S. L. Chuang, K. M. Geib, A. J. Fischer, and A. A. Allerman, "Single-transverse-mode vertical-cavity lasers under continuous and pulsed operation," *IEEE Photon. Technol. Lett.*, vol. 13, no. 9, pp. 927–929, Sep. 2001.

[4] H. Martinsson, J. A. Vukusic, M. Grabherr, R. Michalzik, R. Jager, K. J. Ebeling, and A. Larsson, "Transverse mode selection in large-area oxide-confined vertical-cavity surface-emitting lasers using a shallow surface relief," *IEEE Photon. Technol. Lett.*, vol. 11, no. 12, pp. 1536–1538, Dec. 1999.

[5] H. J. Unold, S. W. Z. Mahmoud, R. Jager, M. Kicherer, M. C. Riedl, and K. J. Ebeling, "Improving single-mode VCSEL performance by introducing a long monolithic cavity," *IEEE Photon. Technol. Lett.*, vol. 12, no. 8, pp. 939–941, Aug. 2000.

[6] D. S. Song, S. H. Kim, H. G. Park, C. K. Kim, and Y. H. Lee, "Single-fundamental-mode photonic-crystal vertical-cavity surface-emitting lasers," *Appl. Phys. Lett.*, vol. 80, pp. 3901–3903, 2002.

[7] N. Yokouchi, A. J. Danner, and K. D. Choquette, "Two-dimensional photonic crystal confined vertical-cavity surface-emitting lasers," *IEEE J. Sel. Topics Quantum Electron.*, vol. 9, no. 5, pp. 1439–1445, Sep. 2003.

[8] N. Yokouchi, A. J. Danner, and K. D. Choquette, "Etching depth dependence of the effective refractive index in two-dimensional photonic-crystal-patterned vertical-cavity surface-emitting laser structures," *Appl. Phys. Lett.*, vol. 82, no. 9, pp. 1344–1346, 2003.

[9] A. J. Danner, J. J. Raftery,Jr., T. Kim, P. O. Leisher, A. V. Giannopoulos, and K. D. Choquette, "Progress in photonic crystal vertical cavity lasers," *IEICE Trans. Electron.*, vol. E88-C, no. 5, pp. 944–950, May 2005.

[10] A. J. Danner, T. S. Kim, and K. D. Choquette, "Single fundamental mode photonic crystal vertical cavity laser with improved output power," *Electron. Lett.*, vol. 41, no. 6, pp. 325–326, 2005.

[11] H. P. D. Yang, F. I. Lai, Y. H. Chang, H. C. Yu, C. P. Sung, H. C. Kuo, S. C. Wang, S. Y. Lin, and J. Y. Chi, "Singlemode (SMSR >40 dB) proton-implanted photonic crystal vertical-cavity surface emitting lasers," *Electron. Lett.*, vol. 41, no. 6, pp. 326–328, 2005.

[12] A. Furukawa, S. Sasaki, M. Hoshi, A. Matsuzono, K. Moritoh, and T. Baba, "High-power single-mode vertical-cavity surface-emitting lasers with triangular holey structure," *Appl. Phys. Lett.*, vol. 85, pp. 5161–5163, 2004.

[13] P. O. Leisher, A. J. Danner, J. J. Raftery,Jr., and K. D. Choquette, "Proton implanted single mode holey vertical-cavity surface emitting lasers," *Electron. Lett.*, vol. 41, no. 18, pp. 1010–1011, 2005.

[14] K. L. Lear, K. D. Choquette, R. P. Schneider,Jr., and S. P. Kilcoyne, "Modal analysis of a small surface emitting laser with a selectively oxidized waveguide," *Appl. Phys. Lett.*, vol. 66, no. 20, pp. 2616–2618, 1995.

[15] E. W. Young, K. D. Choquette, J.-F. P. Seurin, S. L. Chuang, K. M. Geib, and A. A. Allerman, "Comparison of wavelength splitting for selectively oxidized, ion implanted, and hybrid vertical-cavity surface-emitting lasers," *IEEE J. Quantum Electron.*, vol. 39, no. 5, pp. 634–639, Apr. 2003.

[16] V. de Lange, K. Sun, and R. Gordon, "Inside vertical-cavity surface-emitting lasers: Extracting the refractive index from spatial-spectral mode images," *IEEE J. Quantum Electron.*, vol. 43, no. 3, pp. 225–229, Mar. 2007.

[17] P. O. Leisher, A. J. Danner, J. J. Raftery,Jr., D. F. Siriani, and K. D. Choquette, "Loss and index guiding in single mode proton-implanted holey vertical-cavity surface-emitting lasers," *IEEE J. Quantum Electron.*, vol. 42, no. 10, pp. 1091–1096, Oct. 2006.

[18] J.-H. Baek, D.-S. Song, I.-K. Hwang, K.-H, Lee, and Y. H. Lee, "Transverse mode control by etch-depth tuning in 1120-nm GaInAs/GaAs photonic crystal vertical-cavity surface-emitting lasers," *Opt. Exp.*, vol. 12, no. 5, pp. 859–867, 2004.

[19] P. Bienstman, R. Baets, J. Vukusic, A. Larsson, M. J. Noble, M. Brunner, K. Gulden, P. Debernardi, L. Fratta, G. P. Bava, H. Wenzel, B. Klein, O. Conradi, R. Pregla, S. A. Riyopoulos, J.-F. P. Seurin, and S. L. Chuang, "Comparison of optical VCSEL models on the simulation of oxide-confined devices," *IEEE J. Quantum Electron.*, vol. 37, no. 12, pp. 1618–1631, Dec. 2001.

[20] K. J. Ebeling, "Analysis of vertical cavity surface emitting laser diodes (VCSEL)," in *Proc. 15th Scottish Univ. Summer School Phys. Semiconductor Quantum Optoelectron. Quantum Phys. Smart Devices.*, 1999, pp. 295–338.

[21] J.-F. P. Seurin and S. L. Chuang, "Efficient optical modeling of VCSELs using a vector mode-matching method," *Proc. Inst. Electr. Eng. Optoelecton.*, vol. 149, pp. 174–181, 2002.

[22] G. P. Bava, P. Debernardi, and L. Fratta, "Three-dimensional model for vectorial fields in vertical-cavity surface-emitting lasers," *Phys. Rev. A*, vol. 63, pp. 1–13, 2001, 023816.

[23] T. Czyszanowski, M. Dems, and K. Panajotov, "Single mode condition and modes discrimination in photonic-crystal 1.3 μm AlInGaAs/InP VCSEL," *Opt. Exp.*, vol. 15, no. 9, pp. 5604–5608, 2007.

[24] T. Czyszanowski, M. Dems, and K. Panajotov, "Optimal parameters of photonic crystal vertical-cavity surface-emitting diode lasers," *J. Lightw. Technol.*, vol. 25, no. 9, pp. 2331–2336, Sep. 2007.

[25] A. M. Kasten, J. D. Sulkin, P. O. Leisher, D. K. McElfresh, D. Vacar, and K. D. Choquette, "Manufacturable photonic crystal single mode and fluidic vertical cavity surface emitting lasers," *J. Sel. Topics Quantum Electron.*, vol. 14, no. 4, pp. 1123–1131, Jul./Aug. 2008, 2008.

[26] G. R. Hadley, "Effective index model for vertical-cavity surface-emitting lasers," *Opt. Lett.*, vol. 20, no. 13, pp. 1483–1485, 1995.

[27] H. Wenzel and H.-J. Wünsche, "The effective frequency method in the analysis of vertical-cavity surface-emitting laser," *IEEE. J. Quantum Electron.*, vol. 33, no. 7, pp. 1156–1162, Jul. 1997.

[28] A. J. Danner, J. J. Raftery,Jr., P. O. Leisher, and K. D. Choquette, "Single mode photonic crystal vertical cavity lasers," *Appl. Phys. Lett.*, vol. 88, pp. 091114-1–091114-3, 2006.

[29] B. E. A. Saleh and M. C. Teich, *Fundamentals of Photonics*. New York: Wiley, 1991.

[30] A. E. Siegman, "Propagating modes in gain-guided optical fibers," *J. Opt. Soc. Amer. A*, vol. 20, no. 8, pp. 1617–1628, 2003.

[31] L. A. Coldren and S. W. Corzine, *Diode Lasers and Photonic Integrated Circuits*. New York: John Wiley & Sons, Inc., 1995.

[32] T. Czyszanowski, M. Dems, and K. Panajotov, "Impact of the hole depth on the modal behaviour of long wavelength photonic crystal VCSELs," *J. Phys. D, Appl. Phys.*, vol. 40, pp. 2732–2735, 2007.

Dominic F. Siriani (S'07) received the B.S. and M.S. degrees in electrical engineering in 2006 and 2007, respectively, from the University of Illinois, Urbana-Champaign, where he is currently working toward the Ph.D. degree in electrical engineering.

His current research interests include photonic crystal vertical-cavity surface-emitting lasers (VCSELs) and VCSEL arrays.

Mr. Siriani is a student member of the IEEE Photonics Society (formerly the Lasers and Electro-Optics Society). He is a fellow of the National Science Foundation and the National Defense Science and Engineering Graduate.

Paul O. Leisher (S'98–M'07) received the B.S. degree in electrical engineering from Bradley University, Peoria, IL, in 2002 and the M.S. and the Ph.D. degrees in electrical and computer engineering from the University of Illinois at Urbana-Champaign, Urbana, in 2004 and 2007, respectively.

In 2007, he joined nLight Corporation, Vancouver, WA, where he is currently a Device Engineer. His research interests include the design, fabrication, characterization, and analysis of semiconductor lasers and other photonic devices. He has authored or coauthored more than 60 technical journal articles and conference presentations.

Dr. Leisher is a member of the IEEE Photonics Society (formerly the Lasers and Electro-Optics Society) and the Optical Society of America.

Kent D. Choquette (M'97–SM'02–F'03) received the B.S. degree in engineering physics and applied mathematics from the University of Colorado-Boulder, Boulder and the M.S. and the Ph.D. degrees in materials science from the University of Wisconsin-Madison, Madison.

From 1990 to 1992, he was a Postdoctoral Fellow at AT&T Bell Laboratories, Murray Hill, NJ. He then joined Sandia National Laboratories in Albuquerque, NM. From 1993 to 2000, he was a Principal Member of the Technical Staff. Sine 2000, he has been a Professor in the Electrical and Computer Engineering Department, University of Illinois, Urbana-Champaign. He has authored more than 200 technical publications and three book chapters, and has presented numerous invited talks and tutorials.

Prof. Choquette is a Fellow of the Optical Society of America and the International Society for Optical Engineers. He has been an Associate Editor of the IEEE JOURNAL OF QUANTUM ELECTRONICS and IEEE PHOTONIC TECHNOLOGY LETTERS, and a Guest Editor of the IEEE JOURNAL OF SELECTED TOPICS IN QUANTUM ELECTRONICS. From 2000 to 2002, he was an IEEE Lasers and Electro-Optics Society (LEOS, now the Photonics Society) Distinguished Lecturer. He received the 2008 IEEE LEOS Engineering Achievement Award.